

Catalysis of the electrochemical reduction of carbon dioxide†

Cite this: *Chem. Soc. Rev.*, 2013, **42**, 2423

Cyrille Costentin, Marc Robert and Jean-Michel Savéant*

The direct and catalyzed electrochemistry of CO₂ partake in the contemporary attempts to reduce this inert molecule to fuels by means of solar energy, either directly, after conversion of light to electricity, or indirectly in that all elements of comprehension derived from electrochemical experiments can be used in the design and interpretation of photochemical experiments. Following reviews of the activity in the field until 2007–2008, the present review reports more recent findings even if their interpretation remains uncertain. It also develops useful notions that allow analyzing and comparing more rigorously the performances of existing catalysts when the necessary data are available. Among the general trends that transpire presently and are likely to be the object of active future work emphasis is put on the favorable role of acid addition in homogeneous catalytic systems and on the crucial chemical role of the electrode material in heterogeneous catalysis.

Received 30th August 2012

DOI: 10.1039/c2cs35360a

www.rsc.org/csr

1 Introduction

Among the contemporary energy objectives, the reduction of carbon dioxide is a major issue. Ideally, one dreams to convert CO₂ into fuels by means of solar energy. One way is to directly use light to achieve this conversion. The other involves the preliminary conversion of light into electricity and then the electrochemical reduction of CO₂. The first of these approaches has been the object of recent reviews^{1–3} with particularly noteworthy examples.^{4,5} We will therefore concentrate on the electrochemical reduction of CO₂, having however in mind that the data, models and all elements of mechanistic comprehension derived from electrochemical experiments can be used in the design and interpretation of photochemical experiments.

Before addressing the strategies developed for catalyzing the electrochemical reduction of CO₂, it is useful to remind what products are obtained by direct reduction on an electrode material that does not interfere in the reaction and the factors that govern the competition between their formations. This will be the object of the second section of this review.

Direct reduction on such an “outersphere electrode” entails the initial formation of the highly energetic CO₂ anion radical. The standard potential of the CO₂/CO₂^{•−} couple is indeed as

negative as −1.97 V vs. SHE in an aprotic solvent like *N,N'*-dimethylformamide (DMF),⁶ and −1.90 in water.⁷ Catalytic strategies have thus been developed to avoid the intermediacy of the CO₂ anion radical for obtaining the various products one may expect from the electrochemical reduction of CO₂ at lesser energetic costs.⁸ Most of these products appear in the diagram represented in Fig. 1. Not represented on the diagram are multi-carbon products starting with oxalate and other even more important condensation products. Fig. 1 is actually a set of Pourbaix diagrams relating the standard potential of each CO₂ conversion reaction to the pH in water as the solvent, pointing to the fact that in most cases not only electrons but also protons are involved. This observation should be borne in mind when discussing these energetically more favorable strategies, in water as well as in non-aqueous solvents. These strategies essentially consist of catalyzing the target reaction by means of a homogeneous or a heterogeneous catalyst. Homogeneous catalysis has essentially, but not exclusively, involved reduced states of transition metal complexes. Following the pioneering work on Ni and Co macrocyclic complexes as potential catalysts for electrochemical CO₂ reduction,¹⁰ many metal complexes have been used for this purpose. Recent reviews^{11,12} have listed them, sometimes in great detail, until 2007–2008, with however rather cursory descriptions of their performances. In particular, comparison between the various catalysts could not be performed on sound bases. These are the reasons that the present review pursues the following goals: (i) report more recent findings even if their interpretation remains uncertain on the one hand and to analyze and (ii) compare

Université Paris Diderot, Sorbonne Paris Cité, Laboratoire d'Electrochimie Moléculaire, Unité Mixte de Recherche Université – CNRS No 7591, Bâtiment Lavoisier, 15 rue Jean de Baïf, 75205 Paris Cedex 13, France.
E-mail: saveant@univ-paris-diderot.fr

† Part of the solar fuels themed issue.

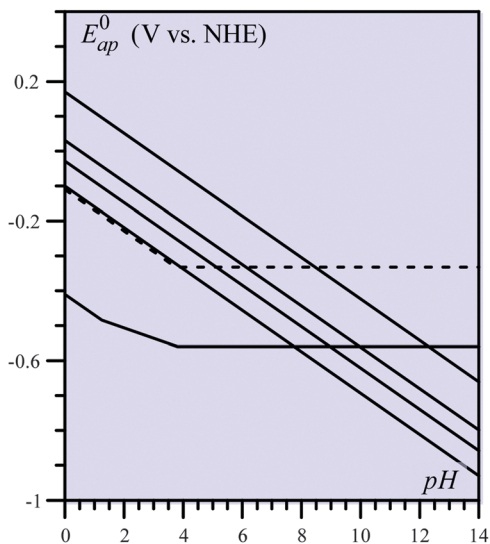
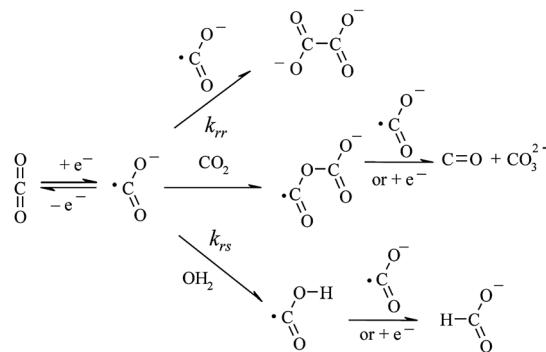


Fig. 1 Variation of the apparent standard potential, E_{ap}^0 , with pH (Pourbaix diagrams) for the reductive conversion of CO_2 into the following products. In the order of decreasing values of E_{ap}^0 at pH = 0: CH_4 , CH_3OH , CH_2O , CO (full line), HCO_2H , HCO_2^- (dashed line), $\text{C}_2\text{O}_4\text{H}_2$, $\text{C}_2\text{O}_4\text{H}^-$, $\text{C}_2\text{O}_4^{2-}$.⁹ The slopes are $R7\ln 10/F$ with the exception of the horizontal lines and of the formation of $\text{C}_2\text{O}_4\text{H}^-$ ($R7\ln 10/2F$).

more rigorously the performances of the catalysts when the necessary data are available. The latter objective requires recalling or describing of some notions that are deemed useful to this purpose. This is the object of Section 3 in which emphasis will be put on the relationships that link turnover frequency and overpotential for preparative scale experiments. It will also describe the way in which cyclic voltammetry can provide an access to these relationships in the framework of a quick catalyst screening. Section 4 reviews the homogeneous catalysts that convert CO_2 essentially to CO (which can be further converted to fuels, like, *e.g.*, methanol or hydrocarbons). The favorable role of acid addition is emphasized and the section closes with an attempt to benchmark the various catalysts described in the literature. Section 5 is devoted to the homogeneous catalysts that give rise to products other than CO , *i.e.*, formate and oxalate. Attempts to produce $\text{CO} + \text{H}_2$ mixtures in prescribed proportions are discussed. The last section is dedicated to heterogeneous catalysts putting emphasis, thanks to a few examples, on the role of the metal of the electrode.

2 Direct electrochemical reduction at inert electrodes

Mercury and lead may be considered as the best approximation of electrode materials that do not interfere in the chemistry of CO_2 reduction. Three products are formed upon electrolysis in DMF at the level of the very negative cyclic voltammetric CO_2 reduction wave,⁶ namely carbon monoxide, oxalate and formate, with a quantitative global faradaic yield. The reaction pathways that lead to these three products are shown



Scheme 1 Reduction of CO_2 at an inert electrode.

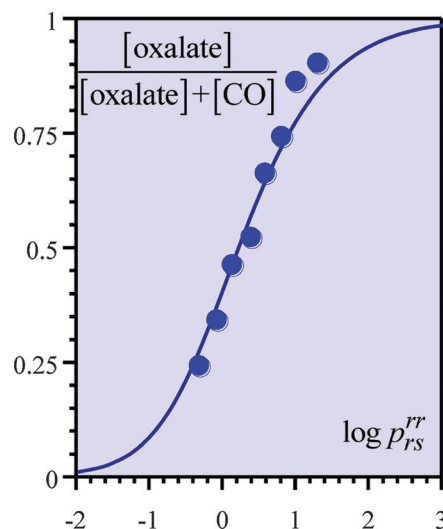


Fig. 2 Oxalate yield in the preparative electrolysis of CO_2 in DMF at a current density of 1.6 mA cm^{-2} at 0°C as a function of CO_2 concentration.¹⁶

in Scheme 1.^{13–16} They are the results of the homogeneous chemistry of the CO_2 anion radical. Dimerization, leading to oxalate, is a manifestation of the radical character of $\text{CO}_2^{\bullet-}$ entailing a one-electron stoichiometry.

CO and carbonate, on the one hand, and formate, on the other, result from $\text{CO}_2^{\bullet-}$ being a Lewis base and a Brønsted base, respectively, leading to a two-electron stoichiometry. The dimerization of the anion radical is fast in DMF⁶ and in water (from pulse radiolysis experiments¹⁷), close to the diffusion limit. This mechanism was substantiated by a careful analysis of the product ratio oxalate/ CO as a function of the concentration of CO_2 . The oxalate/ CO product ratio (in the absence of purposely added water), is an increasing function of the following parameter: $p_{rs}^{rr} = \frac{k_{rr}}{(k_{rs})^{3/2} [\text{CO}_2]^{3/2} D^{1/2} F} I$ (I is the current density, D the CO_2 diffusion coefficient. k_{rr} and k_{rs} are defined in Scheme 1). The good agreement between the theoretical predictions and experiments provides (Fig. 2) a rigorous proof of the mechanism, a rare event in direct and catalyzed electrochemical reduction of CO_2 .

3 Useful notions

We recall in this section notions concerning catalysis in general that may be useful in the mechanism analysis and practical design of catalytic systems for the electrochemical reduction of CO₂. The distinction between redox catalysis and chemical catalysis is not a recently uncovered notion but seems worth recalling each time a booming, and necessarily somewhat anarchic, attention is paid to a new catalysis field as is presently the reduction of CO₂. This is the object of the following first subsection. Re-examining the notion of turnover number, and turnover frequency, and their possible dependence on overpotential is also a timely task for the same reasons. Clarification of these questions in preparative-scale conditions for both heterogeneous and homogeneous catalysis is the object of the following second subsection. Fast screening of the catalytic properties of molecules by means of a non-destructive technique such as cyclic voltammetry, serving as guidelines for preparative-scale electrolyses, is also a timely question, which has recently made significant progresses. This is the object of following third subsection. The notions developed in these two last subsections, provide the bases of meaningful comparison between the various catalytic molecules that have been proposed for the electrochemical reduction of CO₂ as discussed in the following sections.

3.1 Redox and chemical catalysis

In redox catalysis,¹⁸ the catalyst simply shuttles electrons between the electrode and the substrate, acting as an outersphere electron transfer reagent. The very reason that catalysis is obtained is more physical than chemical: the electrons to be transferred are dispersed in a three-dimensional space instead of being confined within a two-dimensional space. Electrochemists are keen designing porous electrodes, so porous that they are sometimes named “volumic electrodes”. Redox catalysis is the equivalent of such an electrode where “volumization” reaches the molecular scale.

In contrast with redox catalysis, where the catalyst acts as an outersphere electron transfer agent, chemical catalysis involves more intimate interactions between the active form of the catalyst and the substrate. Two situations may arise according to the strength of these interactions. In the first of these, bonded interactions in the transition state confer to electron transfer an innersphere character, which results in a lower activation energy than for an outersphere electron transfer of same driving force (Fig. 3). Stronger interactions may involve the formation of an adduct (Fig. 3), which should not however be too stable for an efficient catalysis to operate.

Among others, the reductive conversion of vicinal dihalides into the corresponding olefins has provided a particularly clear illustration of redox and chemical catalysis.^{19,20} In the case of CO₂ reduction, unambiguous examples of redox catalysis could not be established because of deactivation of the catalyst in the course of the catalytic process. Indeed, aromatic molecules, the anion radicals of which usually serve as redox catalysts, undergo carboxylation, preventing them to act as electron mediators. A noteworthy exception to this rule is provided by aromatic

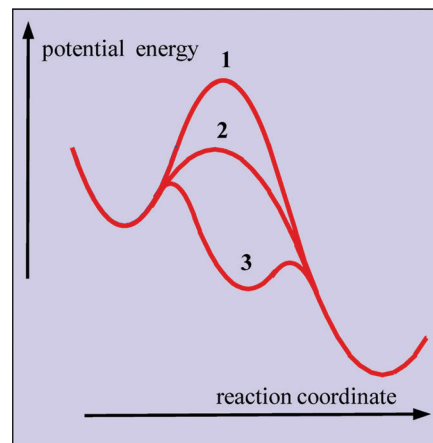


Fig. 3 Redox and chemical catalysis of electrochemical reactions. 1: redox catalysis, 2: one-step chemical catalysis, 3: two-step chemical catalysis.

esters and nitriles, which give rise to a quasi-redox catalysis leading exclusively to oxalate.²¹

3.2 Overpotential and turnover frequency in homogeneous and heterogeneous catalysis²²

The reaction sequence depicted in Scheme 2, complemented with the condition $k' \gg k$, represents an almost general two-electron stoichiometry reaction scheme.²³ The catalytic current in preparative-scale electrolysis then results from the combination of electrode electron transfers, chemical reactions and steady-state linear diffusive transport sketched in Fig. 4, for both heterogeneous catalysis (where a film of catalytic molecules has been deposited on the electrode surface) and homogeneous catalysis (where the catalytic molecules are dispersed in the whole cell compartment).^{24,25} It follows that:

$$\frac{dC_C^b}{dt} = -\frac{SD_A}{V} \left(\frac{dC_C}{dx} \right)_{x=\delta} = \frac{IS}{2FV}$$

In practically interesting systems, the catalytic reaction is fast, in which case: $\frac{I}{2F} = kC_A^0 \Gamma_Q$ in the heterogeneous case and

$$\frac{I}{F} = \sqrt{2kC_A^0 D_P} (C_Q)_{x=0} \text{ in the homogeneous case.}$$

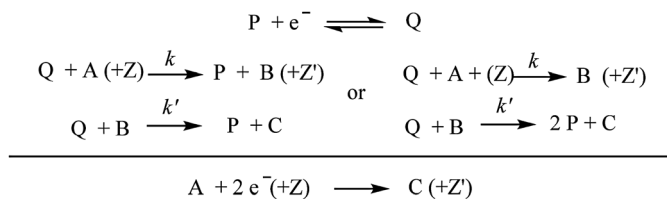
Using the classical definition of the turnover number, TON, as the ratio between the number of molecules transformed by the catalytic reaction and the number of catalyst molecules employed to achieve this transformation, one obtains in the heterogeneous case:

$$\text{TON} = \frac{\text{mol } C}{\text{mol}(P + Q)} = \frac{C_C^b \times V}{\Gamma_P^0 \times S} = kC_A^0 \frac{\Gamma_Q}{\Gamma_P^0} \times t \quad (1)$$

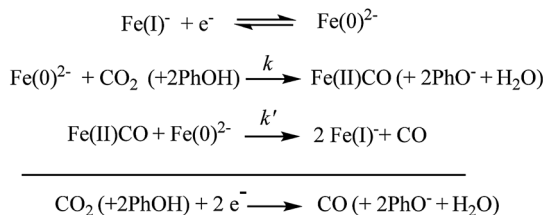
and thus, the turnover frequency:

$$\text{TOF} = kC_A^0 \frac{\Gamma_Q}{\Gamma_P^0} \quad (2)$$

In the homogeneous case, the above expression of the current density is valid for fast catalytic processes, such as the ones of



as for example the reduction of CO_2 into CO catalyzed by iron(0) porphyrins (see Section 4)



Z and Z' are co-reactants or set of co-reactants whose concentration is kept constant during the course of the reaction as for example phenol, phenoxide ion and water in the second reaction scheme. The bimolecular overall rate constant k thus include these constant concentrations

Scheme 2 General two-electron stoichiometry catalytic reaction scheme (P/Q: catalyst couple, A substrate, C product, B: intermediate).

interest in the present discussion. Then “pure kinetic conditions” are achieved corresponding to the establishment, close to the electrode surface, of a steady-state, which results from the mutual compensation of catalytic reaction and catalyst diffusion:

$$D_P \frac{d^2 C_Q}{dx^2} - 2kC_A^0 C_Q = 0,$$

with $(C_Q)_{x=\infty} = 0$, $\left(\frac{dC_Q}{dx}\right)_{x=\infty} = 0$

Within this reaction–diffusion layer, the Q -profile, obtained by space integration of the above differential equation and boundary conditions is:

$$C_Q(x) = (C_Q)_{x=0} \exp\left(-\sqrt{\frac{2kC_A^0}{D_P}} x\right)$$

corresponding to an approximate thickness $\mu = \sqrt{D_P/2kC_A^0}$. Keeping the same definition of TON as in the case of heterogeneous catalysis, we consider the total amount of the catalyst, including both forms, per unit surface area in the reaction layer:

$$\text{mol}(P + Q)_\mu = S \sqrt{\frac{D_P}{2kC_A^0}} C_P^0$$

leading to exactly the expressions of TON and TOF similar but not identical to their heterogeneous counterparts (eqn (1) and (2), respectively):

$$\text{TON} = \frac{\text{mol } C}{\text{mol}(P + Q)_\mu} = kC_A^0 \frac{(C_Q)_{x=0}}{C_P^0} \times t \quad (1')$$

$$\text{TOF} = kC_A^0 \frac{(C_Q)_{x=0}}{C_P^0} \quad (2')$$

Counting only the catalyst molecules present in the reaction layer is the basis of a fair and meaningful comparison between the performances of heterogeneous and homogeneous catalysts. This approach is at variance with current practice, which takes instead the catalyst present in the whole solution into account in the determination of the TON and TOF (see Section 4). This not only unduly disadvantages homogeneous catalysis toward heterogeneous catalysis, but also does not reflect the actual properties of the catalyst. The volume-to-surface ratio of the cell would then interfere, making the comparison between the various reports meaningless. We note that the catalysts present in the solution outside the reaction layer may serve as a useful stock when deactivation of the catalyst in the course of electrolysis occurs, a possibility that is not available in heterogeneous catalysis.

In a number of cases, electron transfer between the electrode and the catalyst is so fast that the Nernst law is obeyed. Then, in both the heterogeneous and homogeneous cases:

$$\text{TOF} = \frac{kC_A^0}{1 + \exp[f(E - E_{\text{cat}}^0)]} \quad (3)$$

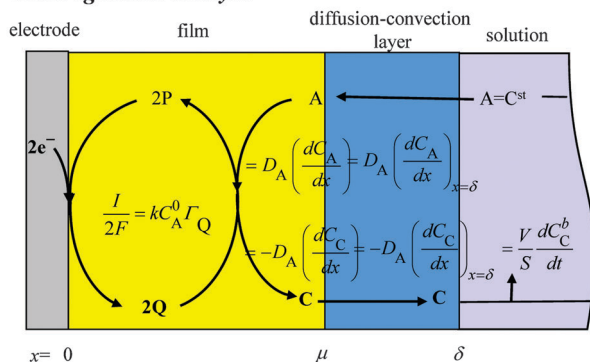
where $f = F/RT$ and E_{cat}^0 is the catalyst standard potential, *i.e.* the standard potential of the P/Q couple.

In a more general case the kinetics of electron transfer to the catalyst is not so fast and may therefore interfere. Then, assuming the validity of the Butler–Volmer rate law with a 0.5 transfer coefficient:²⁷

$$\frac{F}{I} = \frac{1}{2kC_A^0 \Gamma_P^0 \exp[-f(E - E_{\text{cat}}^0)]} + \frac{1}{k_S^{\text{het,cat}} \Gamma_P^0 \exp[-f(E - E_{\text{cat}}^0)/2]} + \frac{1}{2kC_A^0 \Gamma_P^0}$$

in the heterogeneous case, where $k_S^{\text{het,cat}}$ is the heterogeneous electron transfer standard rate constant (corresponding to a

Heterogeneous Catalysis



Homogeneous Catalysis

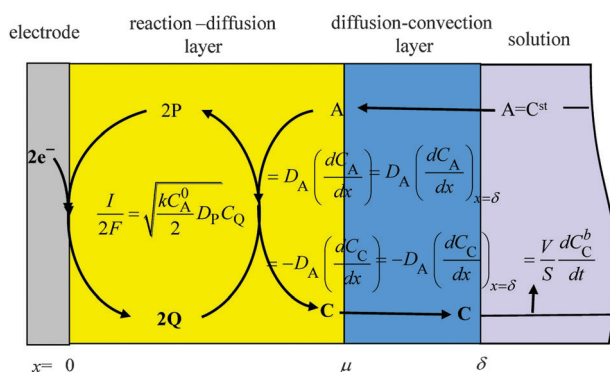


Fig. 4 Catalysis of electrochemical reactions. Electrode electron transfer, chemical reactions and steady state linear diffusive transport in heterogeneous and homogeneous molecular catalysis of an electrochemical reaction according to Scheme 2 (with $k' \gg k$), in the case where the substrate bulk concentration, C_A^0 , is maintained constant during the whole course of electrolysis.²⁶ x : distance to the electrode surface, μ : film (top) or reaction layer (bottom) thickness, δ : diffusion layer thickness. $D_{\text{substrict}}$: diffusion coefficients. $\Gamma_{\text{substrict}}$: surface concentrations. $C_{\text{substrict}}$: volume concentrations. Γ_P^0 , C_P^0 : total surface and volume concentrations of the catalyst. S : electrode surface area, V : cell compartment volume. I : current density, k : catalytic second order rate constant (see Scheme 2).

reactant attached to the electrode surface, dimension of time^{-1}), and:

$$\frac{F}{I} = \frac{1}{\sqrt{2kC_A^0 D_P C_P^0} \exp[-f(E - E_{\text{cat}}^0)]} + \frac{1}{k_S^{\text{cat}} C_P^0 \exp[-f(E - E_{\text{cat}}^0)/2]} + \frac{1}{\sqrt{2kC_A^0 D_P C_P^0}}$$

in the homogeneous case, where k_S^{cat} is the electron transfer standard rate constant corresponding to a reactant in solution (dimension of $\text{space} \times \text{time}^{-1}$)

If the overpotential, η , defined as $\eta = E_{\text{AC}}^0 - E$ (where E is the electrode potential at which electrolysis is run and E_{AC}^0 the standard potential corresponding to the transformation of the substrate A into the product C), is introduced in the preceding equations:

in the heterogeneous case:

$$\frac{1}{\text{TOF}} = \frac{\exp(-f\eta)}{\text{TOF}_0} + \frac{2\sqrt{kC_A^0} \exp\left(-\frac{f\eta}{2}\right)}{k_S^{\text{het,cat}} \sqrt{\text{TOF}_0}} + \frac{\exp[-f(E_{\text{AC}}^0 - E_{\text{cat}}^0)]}{\text{TOF}_0} \quad (4)$$

and in the homogeneous case:

$$\frac{1}{\text{TOF}} = \frac{\exp(-f\eta)}{\text{TOF}_0} + \frac{\sqrt{2D_P} \exp\left(-\frac{f\eta}{2}\right)}{k_S^{\text{cat}} \sqrt{\text{TOF}_0}} + \frac{\exp[-f(E_{\text{AC}}^0 - E_{\text{cat}}^0)]}{\text{TOF}_0} \quad (5)$$

with:

$$\text{TOF}_0 = kC_A^0 \exp[-f(E_{\text{AC}}^0 - E_{\text{cat}}^0)]$$

in both cases.

It thus appears that there is a definite relationship between turnover frequency and overpotential for each particular catalyst. This recently emerged concept allows a precise comparison between catalysts in contrast with the previous notion that each catalyst was characterized by two independent parameters, its TOF and its overpotential, leading to the rather trivial aphorism that a good catalyst is characterized by a large TOF and a small η and *vice versa*. An example of the log TOF- η curve is shown in Fig. 5, where three linear variation zones can be delineated: independence from η at large values of η , linear variation with an $F/RT \ln 10$ slope at small values of η , and, in between, an $F/2RT \ln 10$ slope linear variation corresponding to the kinetic contribution of electron transfer to the catalyst. The latter segment decreases in size and eventually vanishes as electron transfer becomes faster and faster.

It thus appears that one of the best ways to characterize the intrinsic catalytic properties of a molecule is the value of its TOF_0 , the turnover frequency at overpotential zero.

The low overpotential linear variation zone in eqn (4) may look at first sight as a form of a Tafel plot. A "Tafel plot" is a classical

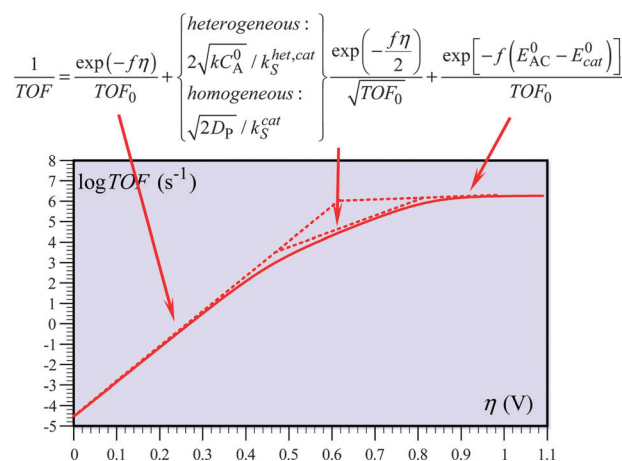


Fig. 5 An example of turnover frequency vs. overpotential relationship.

$$E_{\text{AC}}^0 - E_{\text{cat}}^0 = 0.64 \text{ V}, \log \text{TOF}_0 (\text{s}^{-1}) = -4.6, \sqrt{2D_P}/k_S = 2\sqrt{kC_A^0/k_S^{\text{het,cat}}} = 0.03 \text{ s}^{1/2}.$$

linear approximation of the relationship between the current, or current density, and the overpotential of an electrochemical reaction, kinetically controlled by electron transfer. It is characterized by a transfer coefficient, α , giving rise to the slope $\alpha F/RT \ln 10$ and an exchange current density I_0 defined as the current density at zero overpotential. In the present heterogeneous case:

$$\alpha = 1 \text{ and } I_0/2F = kC_A^0 \Gamma_P^0 \exp[-f(E_{AC}^0 - E_{cat}^0)] \\ = \text{TOF}_0 \times \Gamma_P^0$$

It is seen that, unlike TOF_0 , I_0 is not a molecular intrinsic expression of the catalytic capabilities of the catalyst since it depends on the amount of catalyst one has been able to deposit on the electrode surface. Moreover, Tafel plots with unity transfer coefficients are quite rare for electrochemical reactions kinetically controlled by electron transfer. This recalls to us that eqn (5) is not an actual Tafel plot. It is rather a turnover frequency *vs.* overpotential plot characterizing a deposited molecular catalyst in the low overpotential region.

Likewise in the homogeneous case where:

$$I_0/F = \sqrt{2D_P/kC_A^0} C_P^0 \times \text{TOF}_0,$$

eqn (5) and the plots in Fig. 5, 8 and 10 are not actual Tafel plots.

3.3 Analysis of catalytic responses in cyclic voltammetry

Carrying out a systematic series of electrolyses to evaluate a catalyst, determine the best conditions of its use, avoiding side-phenomena such as ohmic losses, self-inhibition, deactivation *etc.* is an exhausting task. This is the reason that non-destructive techniques, such as cyclic voltammetry,²⁸ are currently used to rapidly gauge what can be the catalytic significance of a molecule and establish the best conditions for preparative scale electrolyses. In spite of previous attempts to define the potential of the cyclic or rotating-disk electrode voltammogram

to be used to estimate the overpotential and the catalytic efficiency,²⁹ successful strategies, as detailed below, for derivation of the $\text{TOF}-\eta$ relationship from cyclic voltammetric data are recent.²²

In the homogeneous case, Fig. 6 shows a zone diagram depicting the various diffusion/reaction regimes that can be observed by means of cyclic voltammetry according to the various intervening parameters (these have been defined in the caption of Fig. 4, ν is the scan rate).^{30,31} The catalytic systems of interest are those in which k is large enough for the representative point of the system to stand in one of the three upper zones in which “pure kinetic conditions” are achieved. Pure kinetic conditions are exactly the same as already introduced in preparative-scale conditions, corresponding to the same steady-state situation. The most classical cyclic voltammetric response is the S-shaped wave in the upper right-hand zone of Fig. 6, of equation:^{32,33}

$$\frac{i}{FS} = \frac{\sqrt{2kC_A^0 D_P C_P^0}}{1 + \exp[-f(E - E_{cat}^0)]} \quad (6)$$

(i : current, S : electrode surface area). It is independent of scan rate and the reverse trace is identical to the forward trace. This type of response corresponds to a fast catalytic reaction with nevertheless negligible consumption of the substrate in the reaction-diffusion layer, and a fast electron transfer between the catalyst and the electrode. Analysis of experimental results by means of eqn (6) is helped by dividing the catalytic current by the peak current, i_p^0 , of the reversible P/Q wave that is observed in the absence of catalysis (*e.g.* in the absence of substrate):^{34,35}

$$\frac{i_p^0}{FS} = 0.446 \times C_P^0 \sqrt{D_P} \sqrt{f\nu} \quad (7)$$

The normalization procedure that thus consists of replacing eqn (6) by eqn (8):³⁶

$$\frac{i}{i_p^0} = \frac{2.24 \sqrt{\frac{2kC_A^0}{f\nu} C_P^0}}{1 + \exp[f(E - E_{cat}^0)]} \quad (8)$$

is a straightforward manner of avoiding the determination of the catalyst diffusion coefficient and the electrode surface area. A representation of eqn (8) is given in Fig. 7a.

Eqn (6) has been used extensively to measure the global catalytic rate constant and thereof to analyze mechanism through determination of reaction orders in catalyst, CO_2 or molecules favoring catalysis such as protons donors (see Section 4.1).³⁷⁻⁴² Caution has sometimes been taken to use this equation when it is indeed applicable, *i.e.*, when the cyclic voltammetric response is (or is close to) an S-shaped curve independent from the direction of the potential scan and from the scan rate.⁴¹ In a large number of cases it has nonetheless been unduly applied when the catalytic response is peak-shaped and – coming together – scan-rate dependent. The odd situation of a scan-rate dependent catalytic rate “constant” thus arises.⁴⁰ One may consequently wonder what the reliability of reactions orders derived in these conditions is and thereof of the mechanistic conclusions drawn.^{37-40,43-46} Various side-phenomena

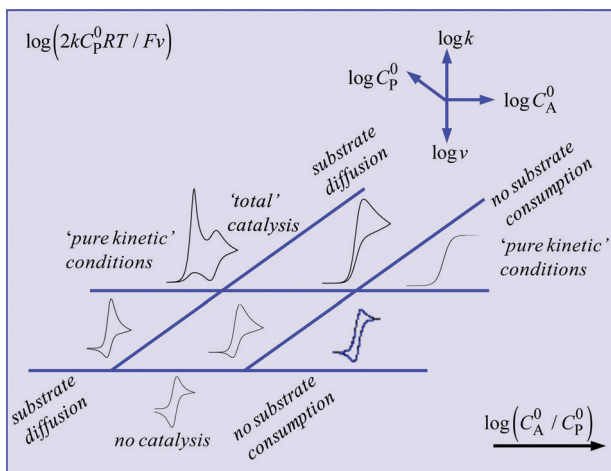


Fig. 6 Diffusion/reaction regimes and shape of the cyclic voltammetric responses in catalytic reactions of the type represented in Scheme 2.

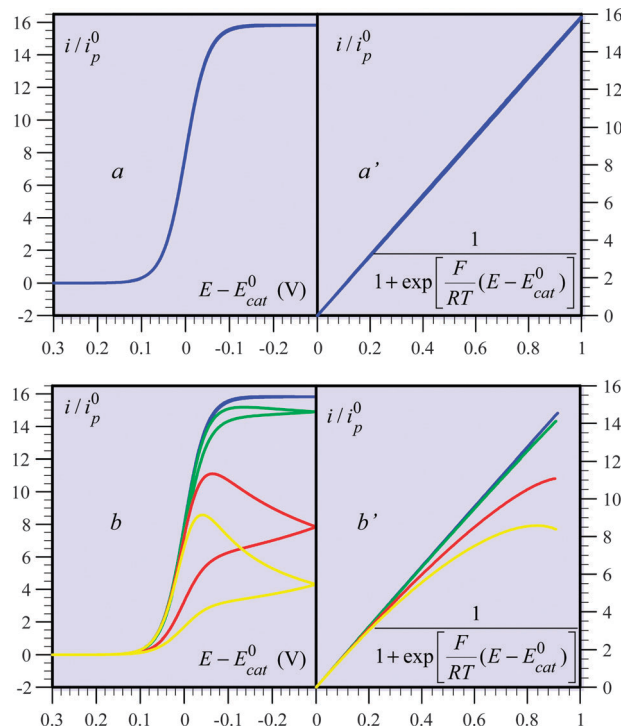


Fig. 7 Catalytic cyclic voltammetry responses (left) and foot-of-the-wave analyses (right) for a typical system, $v = 0.1 \text{ V s}^{-1}$, $D_p = 10^{-5} \text{ cm}^2 \text{ s}^{-1}$, $C_p^0 = 1 \text{ mM}$, $T = 298 \text{ K}$. a, a': $C_A^0 = 1 \text{ M}$, $2k = 100 \text{ s}^{-1}$, no substrate consumption. b, b': substrate consumption. From blue to yellow: $C_A^0 \text{ (M)} = 1, 0.1, 0.01, 0.005$; $2k = 100 \text{ s}^{-1}$.

have been evoked to explain the appearance of a peak-shaped response when an S-shaped response is expected.^{40,47,48}

The most obvious of these side-phenomena is substrate consumption. Passing indeed from the upper-right zone of Fig. 6 to the two left-hand zones entails an increasing consumption of the substrate, the diffusion of which becomes the sole rate-determining step in “total catalysis” conditions. In the intermediate zone, the interference of substrate consumption decreases when one approaches the foot of the catalytic wave. This observation suggests a strategy consisting of plotting i/i_p^0 against $\{1 + \exp[f(E - E_{\text{cat}}^0)]\}^{-1}$. In the case where the catalytic reaction is not perturbed by side phenomena, a straight line is thus obtained over the whole range of $\{1 + \exp[f(E - E_{\text{cat}}^0)]\}^{-1}$, as pictured in Fig. 7a, a'. This is no longer the case if substrate consumption comes into play (Fig. 7b, b'), but remains true at the foot of the wave within an interval that decreases when this side-phenomenon interferes increasingly. The slope of this linear portion may then be used for determining of k and finally of the TOF- η relationship for any catalyst without taking substrate consumption into account. This is due to the fact that at the foot of the wave, the faradaic charge passed is small and therefore the amount of substrate transformed is also small. Raising the scan rate also results in a decrease of the faradaic charge passed in a given potential interval, thus extending the linear portion of the plot.²² There are other phenomena, which may be considered as side-phenomena, *vis à vis* the catalytic reaction, which interfere in an increasing manner as the faradaic

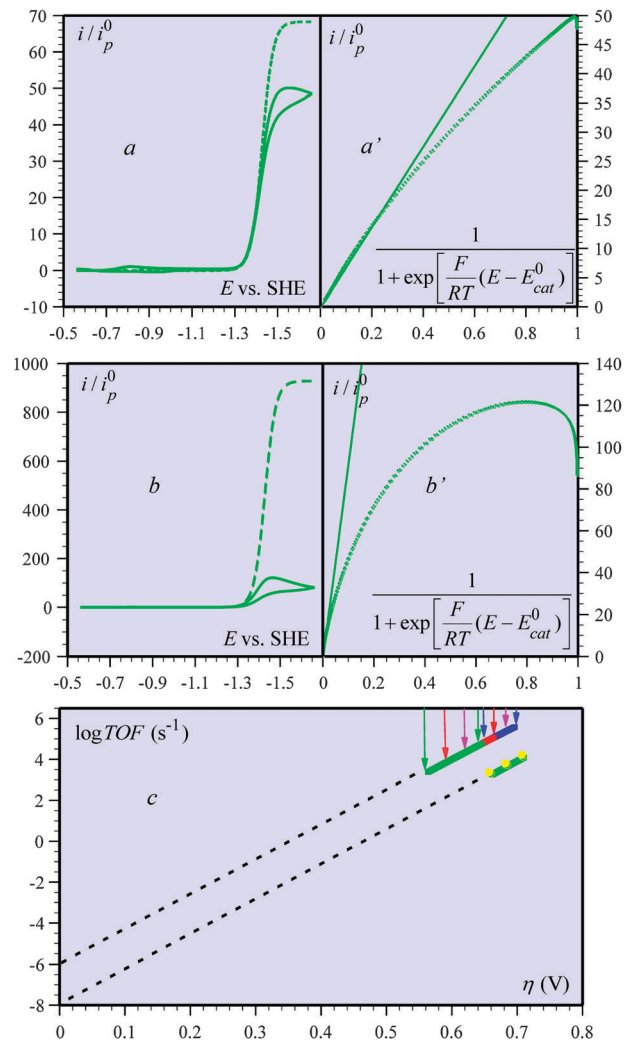


Fig. 8 Catalysis of the electrochemical reduction of CO_2 to CO by electrogenerated Fe(0)TPP . Cyclic voltammetry of FeTPP (1 mM) in $\text{DMF} + 0.1 \text{ M } n\text{-Bu}_4\text{NBF}_4$, in the presence of 0.23 M CO_2 and 0.1 (a, a'), 3 (b, b') M PhOH at a scan rate of 0.1 V s^{-1} . a, b: cyclic voltammetric responses. Solid line: experiments; dashed line: simulation of the corresponding hypothetical unperturbed catalytic responses. a', b': foot-of-the-wave analyses. c: Resulting turnover frequency vs. overpotential relationships (thick lines) derived from the foot-of-the-wave analyses at $0.1, 1, 10, 50 \text{ V s}^{-1}$ (green, red, magenta and blue respectively). The three yellow dots represent the results obtained by means of preparative scale electrolysis in the same conditions as in a.

charge is increased, *e.g.* inhibition by products,⁴⁸ or deactivation of the catalyst.²² The “foot-of-the-wave” strategy applies to these cases too and to any other side-phenomena that interfere increasingly upon increasing the faradaic charge passed.

An illustrative example is given in Fig. 8 where the catalyst for CO_2 -to- CO reduction is electrogenerated iron(0)tetraphenylporphyrin (Fe(0)TPP) in the presence of phenol²² (the favorable role of adding acid will be further discussed in Section 4.1). It is worth noting that the results of preparative-scale electrolysis are consistent with the predictions made on the basis of the foot-of-the-wave analysis, thus validating this strategy.

Extension to the case where electron transfer between the catalyst and the electrode is not unconditionally fast is possible.

This may become necessary even with fast electron exchanging catalysts when catalysis is so fast that electron transfer with the electrode starts to interfere in the overall kinetics. Then, the function that should be plotted against $\{1 + \exp[f(E - E_{\text{cat}}^0)]\}^{-1}$ is no longer i/i_p^0 but, rather:

$$\begin{aligned} \text{FIT}(E - E_{\text{cat}}^0) &= \frac{\frac{i}{i_p^0}}{1 - 0.446 \frac{i_p^0 \sqrt{D_p}}{k_s} \sqrt{f v} \exp\left[\frac{f(E - E_{\text{cat}}^0)}{2}\right]} \\ &= \frac{2.24 \sqrt{\frac{2kC^0}{f v \Delta}}}{1 + \exp\left[\frac{f(E - E_{\text{cat}}^0)}{2}\right]} \end{aligned}$$

k_s is the standard rate constant of electron transfer between the catalyst and the electrode, as derived from the cyclic voltammetry of the catalyst couple in the absence of catalysis. k is then obtained from the slope of the initial linear portion, of the FIT plot, leading finally to the TOF- η relationship. An example of this more sophisticated application of the foot-of-the-wave strategy is given in Section 4.2.

Application of this strategy has two outcomes: (i) determination of the global catalytic rate constants as a function of the concentration of the various reactants, and hence the mechanism of catalysis by means of the reaction orders thus determined; (ii) establishment of the TOF- η relationship as a guide to select the most efficient conditions of preparative-scale electrolysis and to compare the intrinsic properties of the catalysts proposed.

4 Homogeneous catalysis of the reduction of CO₂ to CO

4.1 Favorable role of acids

In the series of palladium-phosphine catalysts, addition of an acid has been shown to be beneficial since the beginning.³⁷⁻⁴² It is remarkable that in spite of the choice of a strong acid, HBF₄, to accelerate CO₂ conversion, CO remains the main product with no or little hydrogen production. In spite of the above-mentioned uncertainties on reaction orders, the mechanism is likely to be of the type shown in Scheme 3 of ref. 42.

Electrogenerated iron(0) porphyrins, essentially tetraphenylporphyrin (TPP) has been shown to be a catalyst for the conversion

of CO₂ to CO.⁴⁹ However, the catalyst deactivates after a few turnovers. Addition of Lewis^{50,51} and Brønsted acids^{47,52} considerably boosts catalysis. In the latter case, weak acids such as alcohols, particularly trifluoroethanol, were used to avoid catalysis of proton reduction as observed with the same Fe(0)TPP, when an acid as strong as Et₃NH⁺ is used.⁵³ It has been shown more recently that addition of moderately strong acids, such as phenols, also boosts catalysis while still yielding essentially CO as product.²² A mechanism, based on reaction orders derived from cyclic voltammetric responses close to the canonical S-shape, has been proposed (Scheme 3 in ref. 47). More reliable and more detailed mechanistic pictures are expected from the systematic application of the foot-of-the-wave analysis of cyclic voltammetric responses as illustrated in Section 3.3 (Fig. 8) with, precisely, the example of phenol addition.⁵⁴

Similar studies of the effect of weak Brønsted acids on the catalysis of the conversion of CO₂ to CO by means of electro-reduced [Re(bpy)(CO)₃(py)]²⁻ have been performed,⁵⁵ in acetonitrile, following the pioneering studies of the Re(bpy)(CO)₃ catalyst.⁵⁶ Mechanistic conclusions were similar to those drawn in the case of Fe(0) porphyrins. The same experiments have been repeated recently⁵⁷ using the same weak Brønsted acids, with determination of reaction orders and of H/D kinetic isotope effects. Application of eqn (8) was considered as safe because the cyclic voltammograms are scan-rate independent even though they do not plateau. In fact, the two characteristics cannot be separated, but the results are most probably reliable because the peaks are very shallow, close to a plateau behavior.

4.2. Attaching the acid groups to the catalyst molecule leads to a very efficient catalysis

Based on the above observations of the favorable role of acids, iron(0) tetraphenylporphyrin with OH substituents in *ortho*, *ortho'* positions of the phenyl groups (Fig. 9, the phenyl groups are in fact perpendicular to the porphyrin ring) proved to be a particularly efficient catalyst of the CO₂ to CO electroreduction.⁵⁸ Fig. 9a shows the very large catalytic current obtained with this molecule. As in many aforementioned cases, it does not plateau off. This is therefore a typical case where the foot-of-the-wave analysis shows its usefulness. The catalysis rate constant can be derived from the linear portion of the plot (Fig. 9b) as well

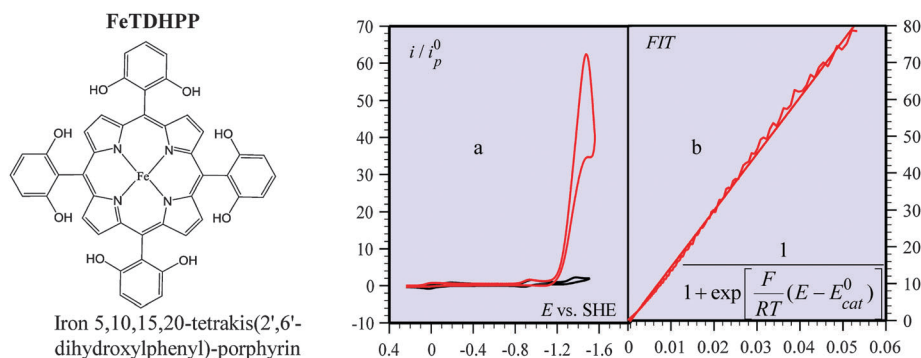


Fig. 9 An iron(0)porphyrin catalyst with the acid groups attached to the molecule. a: cyclic voltammetry of FeTDHPP (1 mM) in DMF + 0.1 M *n*-Bu₄NBF₄, in the absence (black) and presence (red) of CO₂ (0.23 M) at a scan rate of 0.1 V s⁻¹. b: Foot-of-the-wave analysis (see text).

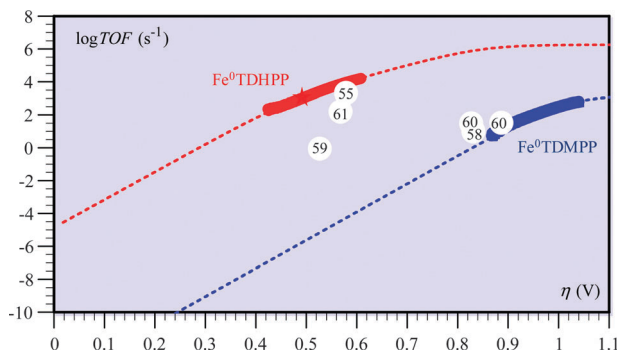


Fig. 10 Correlation between turnover frequency and overpotential for the series of CO₂-to-CO electroreduction catalysts listed in Table 1. Thick red and blue segments: TOF values derived from "foot-of-the-wave-analysis" of the cyclic voltammetric catalytic responses of Fe⁰TDHPP and Fe⁰TDMPP, respectively, in the presence of 2 M H₂O. Dashed lines: plots for Fe⁰TDHPP (top) and Fe⁰TDMPP (bottom). The star indicates a preparative-scale experiment with Fe⁰TDHPP as catalyst.

as the TOF- η relationship. This is shown in Fig. 10 where it is compared to other catalysts of the CO₂ to CO electroreduction (see Section 4.3). Because of the high catalytic rate, electron transfer kinetics between the electrode and the catalyst had to be taken into account in the analysis as detailed in Section 3.3. In this case too, the result of preparative scale electrolysis (star in Fig. 10) falls in line with the prediction of the foot-of-the-wave analysis. That the remarkable catalytic properties of this molecule are related to the presence of the phenolic OH groups in the molecule close to the iron(0) catalytic center is confirmed by comparison with the porphyrin molecule where all the OH groups have been replaced by methoxy substituents (FeTDMPP). Rather high TOF values are also obtained but at the price of a much larger overpotential, resulting in a TOF₀ value one billion times smaller than with FeTDHPP. Comparison with the kinetics of catalysis by Fe(0)TPP in the presence of phenol (Fig. 8c) shows that the eight phenolic groups in Fe(0)TDHPP are equivalent to a 150 M concentration of phenol in solution.

4.3 Catalysts benchmarking

The intrinsic catalytic properties of most of the proposed homogeneous catalysts are compared in Fig. 10, based on the value of the turnover frequency and overpotential as derived from preparative-scale experiments described in the literature (the list is limited to catalysts with a reasonable stability, at least several hours and to electrode materials that do not interfere in the catalytic process). The intrinsic catalytic properties of the various molecules may be compared according to the location of the representative point in the log TOF vs. η plane. The characteristics of each catalyst are summarized in Table 1, in which comparison can also be made through the TOF₀ values. It is seen that the two most efficient catalysts are FeTDHPP and Re(bpy)(CO)₃, with a slight advantage for the former, which also involves a much more common metal than the second.

5 Homogeneous catalysis of the reduction of CO₂ to other products

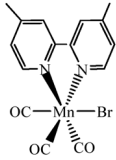

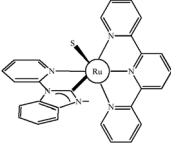
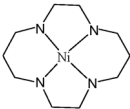
5.1 Formate (vs. CO, vs. H₂)

Formate is also an interesting product since formic acid may be used for hydrogen storage or as a fuel.⁶³ When the reduction of CO₂ takes the anion radical pathway, formate results from the reaction with water and is indeed the only product of electrolysis in water on an inert electrode. In homogeneous catalysis, formate appears as a side-product in many cases but there are catalysts that give a more specific access to its production. For example, substantial amounts of formate were obtained with Rh(diphos)₂ (diphos = 1,2-bis(diphenylphosphino)ethane) as catalyst at a potential where the intermediacy of the rhodium hydride appears likely,⁶⁴ based on previous investigations of the electrochemistry of this complex.⁶⁵ Substantial amounts of formate were obtained together with CO and H₂ with Ru(bpy)₂(CO)₂ as catalyst in acetonitrile or methanol in the presence of a proton donor.⁶⁶ It is interesting to note that the yield in formate increases with the pK_a of the proton donor present. Similarly important yields of formate were also obtained with reduced *cis*-[Rh(bpy)₂X₂]⁺ (X = Cl⁻ or the trifluoromethane-sulfonate anion)⁶⁷ or with another rhodium complex [(η -Me₅C₅)Rh(bpy)Cl]⁺⁶⁸ in acetonitrile. Recent use of the catalyst shown in Scheme 3a, in acetonitrile + 5% water, allowed an even better specificity, with still a non-negligible production of hydrogen (15%).⁶⁹

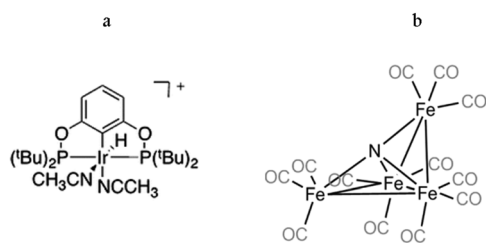
A much better selectivity is obtained when using a tungsten-containing formate dehydrogenase enzyme adsorbed to the electrode surface in water with a high turnover frequency and a very low overpotential.⁷⁰

Several indications from the papers cited above point to a first competition between the addition of CO₂ and of H⁺ on the active reduced form of the catalyst. The former leads to CO and the latter to a metal hydride. The hydride may then react competitively with CO₂ and H⁺, yielding formate and H₂, respectively. One would thus expect that increasing the medium acidity would make the product distribution pass from CO to formate and finally to H₂. This is indeed what seems to happen with the catalyst shown in Scheme 3b.⁷¹ Formate is the "major product" (no figures provided) in the presence of benzoic acid whereas hydrogen is the only product in the presence of the stronger toluenesulfonic acid. In this case, the three cornered competition between CO, formate and H₂ formation under the effect of added acids of various strengths clearly requires further investigation. This is also the case with iron(0) porphyrin, which appears as an excellent catalyst for H₂ evolution in the presence of a strong acid, protonated triethylamine,⁵³ whereas addition of weak (*e.g.* trifluoroethanol), and moderately weak (*e.g.* phenol) acids accelerates the formation of CO. In other words, the conditions for producing syngas mixtures with adjustable proportions of CO and H₂ using a single catalyst are not yet at hand. Another approach to the same goal consists of the combination of two catalyst systems, as in ref. 72 (Re(bpy-*t*Bu)(CO)₃Cl and p-Si under illumination).

Table 1 Catalysis of CO₂ reduction into CO. Correlation between turnover frequency and overpotential for the series of catalysts listed

Solvent $E_{\text{CO}_2/\text{CO}}^0$ (V vs. SHE)	Catalyst E_{cat}^0 (V vs. SHE)	η (V)	log TOF (s ⁻¹)	log TOF ₀ (s ⁻¹)	Ref.
DMF + 2M H ₂ O -0.690	Fe ⁰ TDHPP -1.333	0.41–0.56	2.0–3.9	-4.9	58
	Fe ⁰ TDMPP -1.69	0.89–0.99	1.0–2.2	-14.2	
	Re(bpy)(CO) ₃ -1.25	0.57	3.0	-6.1	
DMF + HBF ₄ -0.260 ^a	{ <i>m</i> -(triphos) ₂ [Pd(CH ₃ CN)] ₂ } -0.76	0.80	0.37	-7.8	59
CH ₃ CN + 5% H ₂ O -0.650	-1.16 	0.51	-0.35	-8.7	60
CH ₃ CN -0.650	-1.30 	0.87	1.2	-9.8	61
	-1.25 	0.81	1.2	-9.1	
1 : 4 H ₂ O CH ₃ CN -0.650	-1.30 	0.55	1.9	-7.4	62

^a The large change in $E_{\text{CO}_2/\text{CO}}^0$ is due to the presence of a strong acid, HBF₄, much stronger than (CO₂ + H₂O).

**Scheme 3** Catalysts for the reduction of CO₂ to formate.

5.2 Oxalate

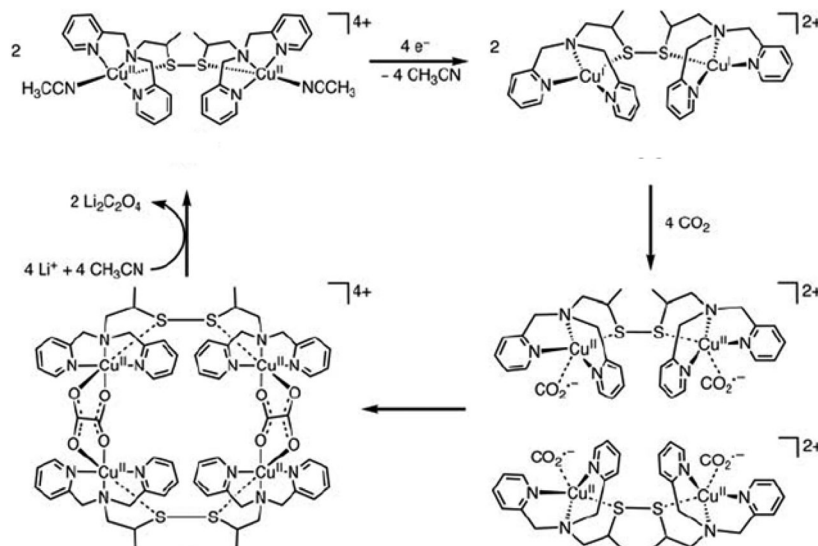
Oxalate is formed in high yields together with CO in the direct reduction of CO₂ on inert electrodes in aprotic media, by means of dimerization of the initial CO₂ anion radical (Section 3). It is formed exclusively in the same medium with anion radicals of aromatic esters and nitriles as catalysts (Section 3.1). In both cases, a rather large overpotential is required to make the reaction go. A remarkable catalytic system in this connection is shown in Scheme 4.⁷³ The formation of oxalate is practically

quantitative in acetonitrile on a glassy carbon electrode at a very low overpotential, prior to the reduction of dioxygen, allowing the capture and reduction of CO₂ from air selectively to a C₂ product, oxalate. It should however be noted that no simple route to reductively transform oxalate or oxalic acid to valuable carbon derivatives is available so far.

6 Heterogeneous catalysis of the reduction of CO₂

6.1 Reduction to CO by means of transition metal complexes at mercury electrodes

In spite of the fact that reduced nickel cyclams have been shown to catalyze the reduction of CO₂ to CO on an inert electrode such as glassy carbon,^{62,74} the same complexes give a much better catalysis on mercury making these systems ones of the most selective and efficient catalysts for the CO₂ to CO conversion.^{75–78} Careful studies have shown that the most likely catalyst is the nickel(I) complex chemisorbed on mercury.^{74,79,80}



Scheme 4 A remarkable catalyst for the reduction of CO_2 to oxalate.

The chemical nature of this adduct and the reasons that make it such a good catalyst are however not known at present. Its surface concentration is likewise unknown making it impossible for the moment a specific characterization of its intrinsic catalytic properties of the type described in Section 3.2 for homogeneous catalysts.

6.2 Reduction in the presence of pyridinium and other organic cations on non-innocent electrodes

Two recently proposed catalytic systems give interesting and puzzling results.

The simpler of the two consists of merely adding to the aqueous solution a large concentration of a salt generally used as an ionic liquid for electrochemical purposes, namely 1-ethyl-3-methylimidazolium tetrafluoroborate in very high concentration (18 mol%). The faradaic yield in CO is practically quantitative, the rate is quite respectable at a rather low overpotential.⁸¹ These spectacular results were interpreted as resulting from a strong interaction between the CO_2 anion radical and the 1-ethyl-3-methylimidazolium cation allowing the formation of the corresponding ion pair at a very positive potential as compared to usual values of the standard potential of the $\text{CO}_2/\text{CO}_2^{\cdot-}$ couple (-1.97 V vs. SHE in an aprotic solvent such as DMF⁶ and -1.90 in water⁷). The influence of ion-pairing on the thermodynamics and kinetics of electrochemical reactions in general is a reasonably well-documented issue (see ref. 82 and 83 and references therein). The peak potentials reported in this study (Fig. S5 and S6 in the supporting information of ref. 81), indicate that the gain in driving force resulting from ion pairing of $\text{CO}_2^{\cdot-}$ by the 1-ethyl-3-methyl imidazolium cation would be of the order of 1.2 eV, implying that electron transfer and ion pairing should be concerted. While such a situation is theoretically conceivable, such a considerable strength of the ion pair is quite unlikely. In the analogous case of the ion pair formed by the superoxide anion radical, taken as a motivation example by the study in ref. 81, the free energy of interaction is not more than

0.07–0.1 eV^{84,85} (the 0.65 eV stabilization mentioned in ref. 81 is for $\text{O}_2^{\cdot-}$ not for O_2^{\cdot}). This is a first clue that the results obtained in ref. 81 are not simply due to ion pairing of $\text{CO}_2^{\cdot-}$ by the 1-ethyl-3-methylimidazolium cation but that the electrode material, platinum or silver, is likely to be involved. The fact that the behavior of an inert electrode such as glassy carbon under the same conditions is not mentioned seems to indicate that the same spectacular results have not been achieved in this case. We may thus conclude that the mechanism of the reaction should be reconsidered in depth having in mind the likely chemical role of the noble metals taken as electrode material. From a practical viewpoint, the fact that noble metals are required as electrode materials tempers the interest of such systems.

Equally interesting and puzzling is the reductive conversion of CO_2 to formic acid/methanol thanks to the addition of protonated pyridine to the solution.^{86–90} A first report mentioned a 30% methanol faradaic yield at a palladium electrode in water at a pH of 5.4 during galvanostatic electrolyses where the electrode potential remains close to -0.5 V vs. SHE in the course of electrolysis.⁸⁶ Formic acid and methanol faradaic yields of 11 and 22% respectively were further reported at platinum or palladium electrode in similar solution and electrolysis conditions.⁸⁸ The rest of the charge passed apparently corresponds to H_2 generation. The replacement of pyridine by 4-*tert*-butylpyridine resulted in the absence of formic acid and of a decreased amount of methanol in the reduction products.⁸⁸ Even better methanol yields, close to 100% are reported on a p-GaP electrode under illumination.⁸⁷ Much lower yields of formic acid (3%) with no methanol formation were recently reported at an illuminated iron pyrite electrode.⁹⁰ It is noteworthy that no such methanol and/or formic acid occurs at a carbon electrode, indicating that some interaction with the electrode material plays an important role.⁸⁸ In spite of this observation detailed mechanism analyses based on cyclic voltammetric responses were carried out as if protonated pyridine was interfering only through homogeneous reactions.^{88,89} Unfortunately most of these analyses were carried out at very low scan rates (5 mV s^{-1})

where the linear diffusion conditions required by the simulations may not be achieved because of the interference of natural convection.⁴⁵ It is remarkable in this respect that when the scan rate is raised to the reasonable value of 0.1 V s^{-1} (Fig. 6 in ref. 89), the wave under examination seems perfectly reversible in the chemical sense and consequently does not contain any usable information about the chemical step associated with electron transfer. We may thus conclude that, at this stage, the mechanism that leads to these interesting results will remain mysterious until the role of the electrode material has been deciphered.^{91,92}

6.3 Copper and copper oxide electrodes

Another example of the importance of the electrode material is provided by the results obtained with copper and copper oxides in water. Copper has long been noticed to be a peculiar and particularly interesting electrode material for CO_2 reduction as allowing the production of methane and even ethylene.^{93–95} The products however vary considerably according to the purity and physical state of the surface as well as to the operating conditions.⁹⁵ CO, formic acid and methanol can indeed be obtained in variable amounts. A recent study reports that electrodes prepared by annealing thick layers of Cu_2O obtained by air oxidation of Cu foils followed by electrochemical reduction of the Cu_2O layer gives much better results in terms of rates and overpotentials than plain Cu electrodes.⁹⁶ The main products were CO and formic acid with a few percents of CH_4 and C_2H_4 . Although these improved performances may be due to the high degree of roughness of the electrodes prepared in this way, it was noted that remaining Cu_2O particles or other Cu^1 species may play an important role. In this respect, catalysis of CO_2 reduction by Cu_2O is well documented, but the product is then methanol.^{97,98} The role of low valent oxides in the reduction of CO_2 also appears important with other metals such as tin.⁹⁹

7. Conclusions and perspectives

As a part of the response to contemporary energy challenges, catalysis of the electrochemical reduction of CO_2 is the object of a current intense attention made of proposition of new systems and re-evaluation of older ones.

In this context, new tools are being made available for characterizing the catalytic properties of the molecules or systems that are proposed. It has been shown that turnover frequency, TOF, and overpotential, η , of molecular catalysts are bound by a defined relationship that depends upon its standard potential, standard rate constant of electron exchange with the electrode and a catalytic kinetic factor that may be expressed as its TOF_0 , *i.e.*, the value of the TOF at zero overpotential. The latter characterization is particularly pertinent for low η values where the TOF– η relationship has the form of a Tafel law. This approach applies to heterogeneous as well as to homogeneous molecular catalysts. A meaningful and fair comparison between the two situations implies taking into account in the definition of turnover numbers and frequencies in the latter case only the

molecules that are contained in the reaction layer adjacent to the electrode and therefore effectively participate in the catalytic process. These notions apply to preparative-scale conditions, *i.e.*, conditions in which the substrate, CO_2 , is effectively converted to the target product as fast as possible with the lowest possible overpotential. Evaluation of the performances of a given catalyst does require that the TOF– η relationship be derived in preparative-scale conditions with minimization of the various side-factors, starting with ohmic drop. For the purpose of catalyst screening such tedious procedures may be replaced by a quicker and simpler approach based on the analysis of the cyclic voltammetric responses of the same catalytic system. As at preparative-scale, various side-phenomena (substrate consumption, catalyst deactivation, self-inhibition *etc.*) affect these responses resulting in deviations from the canonical S-shape curves. These deviations that may be so strong as to result in peak-shaped responses increase as the current increases. They are thus minimized at the foot of the cyclic voltammetric curves. The foot-of-the-wave analysis thus allows a quick derivation of the intrinsic properties of the catalyst. One drawback of the method is that it requires a careful control of the potential scale (ohmic drop, reference electrode drift, *etc.*) precisely because it treats foot-of-the-wave current–potential responses. Having thus derived the intrinsic characteristics of the catalyst one may decide whether or not it is worth considering for preparative scale investigations. Turnover frequency and overpotential may then be selected so as to minimize the same side-phenomena that affect the high-current cyclic voltammetric responses. Particular attention should then be paid to ohmic drop or more generally to the potential distribution at the working electrode surface, which, if not mastered, may result in unexpected competitive product formation. The question of the durability of the catalyst is also essential and can only be treated at the preparative scale. The selection of an anodic reaction is also an important one especially if one wishes to go beyond the laboratory scale.

The most investigated homogeneous systems so far are those that lead to high CO faradaic yields. Application of the above tools has allowed benchmarking of these catalysts.

The favorable role of acid addition has been shown to be important in several cases, leading to an efficient catalyst in which the acid is attached to the molecule itself. However, how these acids interfere in the course of the catalytic reaction remains to be uncovered. Reaction orders analysis susceptible to give the answer should indeed be freed of undue application of relationships that are relevant to the canonical S-shape responses in cases where they are not observed. The foot-of-the-wave analysis is worth considering in these conditions. One could then address by means of systematic investigations, fundamental mechanistic questions. For example, what is the respective role of acid *vs.* H-bonding properties? In the CO_2 -to-CO conversion, how the breaking of one C–O bond is coupled with proton and electron transfer? Proton (P) coupled (C) electron (E) transfer (T) reactions are currently receiving a lot of attention,^{100,101} but so far PCET coupled with heavy atom bond breaking has been fully analyzed only in one case, that of an O–O bond.¹⁰² One may expect an answer to this problem

once the kinetics of relevant steps have been extracted from the global catalysis kinetics.

Homogeneous catalysis by transition metal complexes may be applied to the formation of products other than CO, notably formate and oxalate. Formate may indeed be considered as an interesting intermediate or, directly, for energy storage. In several cases, formate is deemed to result from the reaction of an hydride donor intermediate with CO₂. Systematic investigations aiming at the determination of the factors that govern the respective formation of formate, CO and hydrogen would certainly be welcome. Oxalate is formed specifically with aromatic esters anion radicals as catalysts. It is obtained at a remarkably much lower overpotential – so low that the reduction can be performed in the presence of dioxygen – by means of a dimeric Cu^I sulfide complex. Reduction of the oxalic acid thus obtained without breaking the C–C bond is a definitely worthwhile objective.

In terms of heterogeneous catalysis of CO₂ reduction, copper is also remarkable as an electrode material in the sense that methane and even ethylene may be obtained. Other interesting products may also be obtained and the role of Cu^I oxide has been emphasized either as a precursor of activated Cu⁰ or, directly, as the catalyst as observed when methanol is the target product.

Methanol is also the main product with the remarkably simple addition of protonated pyridine to the solution. The reaction does not occur on an inert electrode such as glassy carbon, leading to the idea that the electrode material, Pt or GaP under illumination, plays an essential role. The same is true with the addition of a liquid electrolyte, which allows the fast formation of CO at low overpotentials.

The role of the electrode material – mercury in this case – in the remarkable efficiency of nickel cyclam as a catalyst of the CO₂-to-CO conversion, known for a long time, also transpires in recent studies in the area.

Overall, good theoretical and empirical starting points exist but much work remains to be done before mechanisms are clarified and efficient practical procedures are designed.

References

- H. Takeda and O. Ishitani, *Coord. Chem. Rev.*, 2010, **254**, 346–354.
- D. Windle and R. N. Perutz, *Coord. Chem. Rev.*, 2012, **256**, 2562–2570.
- Y. Izumi, *Coord. Chem. Rev.*, DOI: 10.1016/j.ccr.2012.04.018.
- T. W. Woolerton, S. Sheard, E. Reisner, E. Pierce, S. W. Ragsdale and F. A. Armstrong, *J. Am. Chem. Soc.*, 2010, **132**, 2132–2133.
- M. A. Méndez, P. Voyame and H. H. Girault, *Angew. Chem., Int. Ed.*, 2011, **50**, 7391–7394.
- E. Lamy, L. Nadjó and J. M. Savéant, *J. Electroanal. Chem.*, 1977, **78**, 403–407.
- H. A. Schwarz and R. W. Dodson, *J. Phys. Chem.*, 1989, **93**, 409–414.
- The use of visible light in photochemical processes, imposes rather stringent constraints in terms of potentials accessible by visible light irradiations of dyes or semiconductors.
- K. W. Frese Jr, in *Electrochemical and Electrocatalytic Reactions of Carbon Dioxide*, ed. B. P. Sullivan, K. Krist and H. E. Guard, Elsevier, New York, ch. 6, 1993.
- B. J. Fisher and R. Eisenberg, *J. Am. Chem. Soc.*, 1980, **102**, 7361–7363.
- J.-M. Savéant, *Chem. Rev.*, 2008, **108**, 2348–2378.
- E. E. Benson, C. P. Kubiak, A. J. Sathrum and J. M. Smieja, *Chem. Soc. Rev.*, 2009, **38**, 89–99.
- C. Amatore and J. M. Savéant, *J. Am. Chem. Soc.*, 1981, **103**, 5021–5023.
- C. Amatore and J. M. Savéant, *J. Electroanal. Chem.*, 1981, **125**, 23–39.
- C. Amatore, L. Nadjó and J. M. Savéant, *New J. Chem.*, 1984, **8**, 565–566.
- A. Gennaro, A. A. Isse, M.-G. Severin, E. Vianello, I. Bhugun and J.-M. Savéant, *J. Chem. Soc., Faraday Trans.*, 1996, **92**, 3963–3968.
- P. Neta, R. E. Huie and A. B. Ross, *J. Phys. Chem. Ref. Data*, 1988, **17**, 1027–1284.
- J.-M. Savéant, *Elements of Molecular and Biomolecular Electrochemistry*, Wiley-Interscience, New York, 2006, ch. 4, pp. 251–252.
- D. Lexa, J. M. Savéant, K. B. Su and D. L. Wang, *J. Am. Chem. Soc.*, 1987, **109**, 6464.
- D. Lexa, J. M. Savéant, H. J. Schäfer, K. B. Su, B. Vering and D. L. Wang, *J. Am. Chem. Soc.*, 1990, **112**, 6162.
- A. Gennaro, A. A. Isse, J. M. Savéant, M. G. Severin and E. Vianello, *J. Am. Chem. Soc.*, 1996, **118**, 7190–7196.
- C. Costentin, S. Drouet, M. Robert and J.-M. Savéant, *J. Am. Chem. Soc.*, 2012, **134**, 11235–11242.
- (a) Scheme 1 is for a reductive process. Transposition to oxidation is straightforward; (b) A stoichiometric factor of 2 was unduly omitted in the derivations and expressions of ref. 22. Correction submitted.
- C. Amatore and J.-M. Savéant, *J. Electroanal. Chem.*, 1981, **123**, 189–201.
- Ref. 18, ch. 2, pp. 132–139.
- Other regimes may be analyzed along the same lines²².
- Ref. 18, ch. 1, pp. 28–32.
- In cyclic voltammetry or in related techniques about one millionth of the substrate is consumed during each run at usual slow scan rates (0.1 V s⁻¹), making these techniques “non-destructive” as opposed to bulk electrolyses, where the objective is instead to transform as much as possible of the substrate in the shortest possible time.
- V. Fourmond, P.-A. Jacques, M. Fontecave and V. Artero, *Inorg. Chem.*, 2010, **49**, 10338–10347.
- J.-M. Savéant and K.-B. Su, *J. Electroanal. Chem.*, 1984, **171**, 341–349.
- Ref. 18, ch. 2, pp. 108–111.
- J.-M. Savéant and E. Vianello, in *Advances in Polarography*, ed. I. S. Longmuir, Pergamon Press, Cambridge, UK, 1959, pp. 367–374.
- J.-M. Savéant and E. Vianello, *Electrochim. Acta*, 1965, **10**, 905–920.
- J. E. B. Randles, *Trans. Faraday Soc.*, 1948, **44**, 327–328.
- A. Sevcik, *Coll. Czech. Chem. Commun.*, 1948, **13**, 349–377.
- C. P. Andrieux, C. Blocman, J.-M. Dumas-Bouchiat, F. M'Halla and J.-M. Savéant, *J. Electroanal. Chem.*, 1980, **113**, 19–40.
- D. L. DuBois, A. Miedaner and R. C. Haltiwanger, *J. Am. Chem. Soc.*, 1991, **113**, 8753–8764.
- P. R. Bernatis, A. Miedaner, R. C. Haltiwanger and D. L. DuBois, *Organometallics*, 1994, **13**, 4835–4843.
- A. Miedaner, B. C. Noll and D. L. DuBois, *Organometallics*, 1997, **16**, 5779–5791.
- D. Steffey, C. J. Curtis and D. L. DuBois, *Organometallics*, 1995, **14**, 4937–4943.
- J. W. Raebiger, J. W. Turner, B. C. Noll, C. J. Curtis, A. Miedaner, B. Cox and D. L. DuBois, *Organometallics*, 2006, **25**, 3345–3351.
- M. Rakowski Dubois and D. L. Dubois, *Acc. Chem. Res.*, 2009, **42**, 1974–1982.
- Another example of similar, and even more severe, inconsistency is the application of the expression of the catalytic plateau, $i/FS = \sqrt{2kC_A^0 D_P C_P^0}$ to the height of a sharp peak, calling this expression, the “Randles-Sevcik equation”, while the actual Randles-Sevcik equation pertains to a simple Nernstian diffusion controlled response (eqn (7)).
- Z. Chen, C. Chen, D. R. Weinberg, P. Kang, J. J. Concepcion, D. P. Harrison, M. S. Brookhart and T. J. Meyer, *Chem. Commun.*, 2011, **47**, 12607–12609.
- Sometimes very low scan rates are used to obtain the expected canonical plateau-shaped wave as, e.g., in ref. 46 where scan rates as low as 2 mV s⁻¹ have been used. In these conditions the plateau shape may as well result from natural convection, which makes the current–potential curves look like rotating disk electrode voltammograms in all circumstances.
- M. D. Rail and L. A. Berben, *J. Am. Chem. Soc.*, 2011, **133**, 18577–18579.
- I. Bhugun, D. Lexa and J.-M. Savéant, *J. Am. Chem. Soc.*, 1996, **118**, 1769–1776.
- I. Bhugun and J.-M. Savéant, *J. Electroanal. Chem.*, 1996, **408**, 5–14.

- 49 M. Hammouche, D. Lexa, J.-M. Savéant and M. Momenteau, *J. Electroanal. Chem.*, 1988, **249**, 347–351.
- 50 M. Hammouche, D. Lexa, M. Momenteau and J.-M. Savéant, *J. Am. Chem. Soc.*, 1991, **113**, 8455–8466.
- 51 I. Bhugun, D. Lexa and J.-M. Savéant, *J. Phys. Chem.*, 1996, **100**, 19981–19985.
- 52 I. Bhugun, D. Lexa and J.-M. Savéant, *J. Am. Chem. Soc.*, 1994, **116**, 5015–5016.
- 53 I. Bhugun, D. Lexa and J.-M. Savéant, *J. Am. Chem. Soc.*, 1996, **118**, 3982–3983.
- 54 Electrogenerated Fe(0)TPP is sometimes given the reputation of having a good current efficiency but requiring a hopelessly large overpotential and to require mercury as the electrode.^{2,11} The TOF- η curve for this catalyst represented in Fig. 8c shows that the first of these assertions is inaccurate. Mercury is not required. The results are closely the same on glassy carbon. Mercury was preferred in most cases because scan-rate dependency investigations are easier than on glassy carbon. The situation is in this sense quite different from that of catalysts for which mercury is essential to their performances as discussed in Section 6.1.
- 55 K.-Y. Wong, W.-H. Chung and C.-P. Lau, *J. Electroanal. Chem.*, 1998, **453**, 161–169.
- 56 J. Hawecker, J. M. Lehn and R. Ziessel, *J. Chem. Soc., Chem. Commun.*, 1984, 328–330.
- 57 M. Smieja, E. E. Benson, B. Kumar, K. A. Grice, C. S. Seu, A. J. M. Miller, J. M. Mayer and C. P. Kubiak, *Proc. Natl. Acad. Sci. U. S. A.*, 2012, **109**, 15646–15650.
- 58 C. Costentin, S. Drouet, M. Robert and J.-M. Savéant, *Science*, 2012, **338**, 90–94.
- 59 J. W. Raebiger, J. W. Turner, B. C. Noll, C. J. Curtis, A. Miedaner, B. Cox and D. L. DuBois, *Organometallics*, 2006, **25**, 3345–3351.
- 60 M. Bourrez, F. Molton, S. Chardon-Noblat and A. Deronzier, *Angew. Chem., Int. Ed.*, 2011, **50**, 9903–9906.
- 61 Z. Chen, C. Chen, D. R. Weinberg, P. Kang, J. J. Concepcion, D. P. Harrison, M. S. Brookhart and T. J. Meyer, *Chem. Commun.*, 2011, **47**, 12607–12609.
- 62 J. D. Froehlich and C. P. Kubiak, *Inorg. Chem.*, 2012, **51**, 3932–3934.
- 63 T. C. Johnson, D. J. Morris and M. Wills, *Chem. Soc. Rev.*, 2010, **39**, 81–88.
- 64 S. Slater and J. H. Wagenknecht, *J. Am. Chem. Soc.*, 1984, **106**, 5367–5368.
- 65 G. Pilloni, E. Vecchi and M. Martelli, *J. Electroanal. Chem.*, 1973, **45**, 483–487.
- 66 H. Ishida, H. Tanaka, K. Tanaka and T. Tanaka, *J. Chem. Soc., Chem. Commun.*, 1987, 131–132.
- 67 C. M. Bolinger, N. Story, B. P. Sullivan and T. J. Meyer, *Inorg. Chem.*, 1988, **27**, 4582–4587.
- 68 C. Caix, S. Chardon-Noblat and A. Deronzier, *J. Electroanal. Chem.*, 1997, **434**, 163–170.
- 69 P. Kang, C. Cheng, Z. Chen, C. K. Schauer, T. J. Meyer and M. Brookhart, *J. Am. Chem. Soc.*, 2012, **134**, 5500–5503.
- 70 T. Reda, C. M. Plugge, N. J. Abram and J. Hirst, *Proc. Natl. Acad. Sci. U. S. A.*, 2008, **105**, 10654–10658.
- 71 M. D. Rail and L. A. Berben, *J. Am. Chem. Soc.*, 2011, **133**, 18577–18579.
- 72 B. Kumar, J. M. Smieja, A. F. Sasayama and C. P. Kubiak, *Chem. Commun.*, 2012, **48**, 272–274.
- 73 R. Angamuthu, P. Byers, M. Lutz, A. L. Spek and E. Bouwman, *Science*, 2010, **327**, 313–315.
- 74 M. Fujihira, Y. Hirata and K. Suga, *J. Electroanal. Chem.*, 1990, **292**, 199–215.
- 75 M. Beley, J. P. Collin, R. Ruppert and J. P. Sauvage, *J. Chem. Soc., Chem. Commun.*, 1984, 1315–1316.
- 76 M. Beley, J. P. Collin, R. Ruppert and J. P. Sauvage, *J. Am. Chem. Soc.*, 1986, **108**, 7461–7467.
- 77 J. P. Collin, A. Jouaiti and J. P. Sauvage, *Inorg. Chem.*, 1988, **27**, 1986–1990.
- 78 J. Schneider, H. Jia, K. Kobihiro, D. E. Cabelli, J. T. Muckerman and E. Fujita, *Energy Environ. Sci.*, 2012, **5**, 9502–9510.
- 79 G. B. Balazs and F. C. Anson, *J. Electroanal. Chem.*, 1992, **322**, 325–345.
- 80 G. B. Balazs and F. C. Anson, *J. Electroanal. Chem.*, 1993, **361**, 149–157.
- 81 B. A. Rosen, A. Salehi-Khojin, M. R. Thorson, W. Zhu, D. T. Whipple, P. J. A. Kenis and R. I. Masel, *Science*, 2011, **334**, 643–644.
- 82 J.-M. Savéant, *J. Phys. Chem. B*, 2001, **105**, 8995–9001.
- 83 J.-M. Savéant, *J. Am. Chem. Soc.*, 2008, **130**, 4732–4741.
- 84 A. S. Barnes, E. I. Rogers, I. Streeter, L. Aldous, C. Hardacre, G. G. Wildgoose and R. G. Compton, *J. Phys. Chem. C*, 2008, **112**, 13709–13715.
- 85 M. Islam and T. Ohsaka, *J. Phys. Chem. C*, 2008, **112**, 1269–1275.
- 86 G. Seshadri, C. Lin and A. B. Bocarsly, *J. Electroanal. Chem.*, 1994, **372**, 145–150.
- 87 E. E. Barton, D. M. Rampulla and A. B. Bocarsly, *J. Am. Chem. Soc.*, 2008, **130**, 6342–6344.
- 88 E. Barton Cole, P. S. Lakkaraju, D. M. Rampulla, A. J. Morris, E. Abelev and A. B. Bocarsly, *J. Am. Chem. Soc.*, 2010, **132**, 11539–11551.
- 89 A. J. Morris, R. T. McGibbon and A. B. Bocarsly, *ChemSusChem*, 2011, **4**, 191–196.
- 90 A. B. Bocarsly, Q. D. Gibson, A. J. Morris, R. P. L'Esperance, Z. M. Detweiler, P. S. Lakkaraju, E. L. Zeitler and T. W. Shaw, *ACS Catal.*, 2012, **2**, 1684–1692.
- 91 Recent quantum chemical calculations of the characteristics of the pyH⁺/pyH* couple conclude that it cannot be involved in the reaction.⁹³ Such calculations were not in fact necessary: it suffices to note that the reaction does not occur at inert electrodes. Moreover these calculations do not seem to reproduce correctly the experimental behavior of pyH⁺ reduction at an inert electrode.
- 92 J. A. Keith and E. A. Carter, *J. Am. Chem. Soc.*, 2012, **134**, 7580–7583.
- 93 Y. Hori, K. Kikuchi and S. Suzuki, *Chem. Lett.*, 1985, 1695–1698.
- 94 Y. Hori, K. Kikuchi, A. Murata and S. Suzuki, *Chem. Lett.*, 1986, 897–898.
- 95 Y. Hori, in *Modern Aspects of Electrochemistry*, ed. C. G. Vayenas, R. E. White and M. E. Gamboa-Aldeco, Springer, New York, 2008, vol. 42, p. 89.
- 96 C. W. Li and M. W. Kanan, *J. Am. Chem. Soc.*, 2012, **134**, 7231–7234.
- 97 K. W. Frese, *J. Electrochem. Soc.*, 1991, **138**, 3338–3344.
- 98 M. Le, M. Ren, Z. Zhang, P. T. Sprunger, R. L. Kurtz and J. C. Flake, *J. Electrochem. Soc.*, 2011, **158**, E45–E49.
- 99 Y. Chen and M. W. Kanan, *J. Am. Chem. Soc.*, 2012, **134**, 1986–1989.
- 100 *Chem. Rev.* thematic issue “Proton-Coupled Electron Transfer” 2010, **110**, 6937–7100.
- 101 *Energy Environ. Sci.* themed issue “Proton-Coupled Electron Transfer” 2012, **5**, 7677–7694.
- 102 C. Costentin, V. Hajj, M. Robert, J.-M. Savéant and C. Tard, *Proc. Natl. Acad. Sci. U. S. A.*, 2011, **108**, 8559–8564.